JOC Article

Understanding the Unusual Regioselectivity in the Nucleophilic Ring-Opening Reactions of *gem*-Disubstituted Cyclic Sulfates. Experimental and Theoretical Studies

Alberto Avenoza,*[,†] Jesús H. Busto,[†] Francisco Corzana,[†] José I. García,*[,‡] and Jesús M. Peregrina[†]

Departamento de Química, Universidad de La Rioja, Grupo de Síntesis Química de La Rioja, U.A.-C.S.I.C., E-26006 Logroño, Spain, and Departamento de Química Orgánica, Instituto de Ciencia de Materiales de Aragón, C.S.I.C.-Universidad de Zaragoza, E-50009 Zaragoza, Spain

alberto.avenoza@dq.unirioja.es; jig@posta.unizar.es

Received February 7, 2003

The regioselectivity of the nucleophilic ring-opening reactions of three *gem*-disubstituted cyclic sulfates with sodium azide has been studied from both experimental and theoretical viewpoints. It is found that, depending on the substituent present in the cyclic sulfate, the reaction displays reversed regioselectivity, which allows one or another regioisomer to be obtained with selectivities greater than 4:1. The theoretical calculations show that, contrary to previous understanding, the intrinsic preference in all cases is azide attack at the less-substituted C_β position, a consequence of similar stereoelectronic effects in the three sulfates considered. The observed preference for C_α attack in the case of the ester sulfate is explained in terms of differential solvent effects, which are in turn due to subtle differences in the charge transfer in the different transition structures.

Introduction

The important role of cyclic sulfates in organic synthesis has been described in two recent reviews.[1,2] In particular, five-membered cyclic sulfates compete with epoxides in terms of reactivity and selectivity, and in many cases they are found to be superior to epoxides in opening reactions with nucleophiles.

The development of both the catalytic asymmetric dihydroxylation (AD) reaction[3] (a tool to obtain chiral 1,2-diols) and efficient methods for the preparation of cyclic sulfates from 1,2-diols[1,2,4] have contributed to the expansion of the chemistry of these cyclic compounds.

On the other hand, 1,2-amino alcohols play important roles in medicinal chemistry,[5] coordination chemistry, and asymmetric catalysis.[6] There are a number of reactions, including asymmetric aminohydroxylation (AA),[7] that can be used in the synthesis of enantiopure 1,2-amino alcohols. However, one of the best methods involves the use of 1,2-azido alcohols, which are often obtained by opening of cyclic sulfates with the azide ion followed by hydrolysis, since these compounds have several advantages (good nucleophile, mild reaction conditions, and easy conversion into amine group).[1,2]

Taking into account the observations outlined above, and the fact that most intermolecular ring-opening reactions between cyclic sulfates and nucleophiles proceed by the S_N2 pathway with total inversion at the reacting stereogenic center,[1,2] we focused our attention on the ring opening of cyclic sulfates with the azide ion. A number of general features concerning the regioselectivity of this reaction are well-established and are covered in the aforementioned reviews. The regioselectivity is controlled simultaneously by the steric interaction between the substrates and nucleophiles and by the electronic distribution of the substrates. For example, in monosubstituted α,β-cyclic sulfates in which the substituent is a bulky alkyl group, the nucleophile attacks almost exclusively at the C_β position (sulfate **1a** gives compound **3a**, Scheme 1).[5d,8] Nevertheless, the situation is reversed when the substituent is an electron-withdrawing group, since in this case it is the electronic distribution of the substrate or the transition state rather than the steric hindrance that seems to be the predomi-

† Universidad de La Rioja.
‡ CSIC-Universidad de Zaragoza.

(1) Lohray, B. B. *Synthesis* **1992**, 1035−1052.
(2) Bittman, R.; Byun, H.-S.; He, L. *Tetrahedron* **2000**, *56*, 7051−7091.
(3) Kolb, H. C.; VanNieuwenhze, M. S.; Sharpless, K. B. *Chem. Rev.* **1994**, *94*, 2483−2547.
(4) Lohray, B. B.; Bhushan, V. *Adv. Heterocycl. Chem.* **1997**, *68*, 89−180.
(5) (a) Hannun, Y. *Science* **1996**, *274*, 1855−1859. (b) Byun, H.-S.; Bittman, R. In *Phospholipids Handbook*; Cevc, G., Ed.; Marcel Dekker: New York, 1993; pp 97−140. (c) Lister, M. D.; Ruan, Z.-S.; Bittman, R. *Biochim. Biophys. Acta* **1995**, *1256*, 25−30. (d) Byun, H.-S.; Sadlofsky, J. A.; Bittman, R. *J. Org. Chem.* **1998**, *63*, 2560−2563.
(6) (a) Pu, L.; Yu, H.-B. *Chem. Rev.* **2001**, *101*, 757−824. (b) Noyori, R. *Chem. Soc. Rev.* **1989**, *18*, 187−208. (c) Noyori, R.; Kitamura, M. *Angew. Chem., Int. Ed. Engl.* **1991**, *30*, 49−69. (d) Itsuno, S.; Ito, K.; Hirao, A.; Nakahama, S. *J. Org. Chem.* **1984**, *49*, 555−557. (e) Corey, E. J. *Pure Appl. Chem.* **1990**, *62*, 1209−1216.
(7) (a) Sharpless, K. B.; Bruncko, M.; Schlingloff, G. *Angew. Chem., Int. Ed. Engl.* **1997**, *36*, 1483−1486. (b) Sharpless, K. B.; Tao, B.; Schlingloff, G. *Tetrahedron Lett.* **1998**, *39*, 2507−2510. (c) Song, C. E.; Oh, C. R.; Roh, E. J.; Lee, S.; Choi, J. H. *Tetrahedron: Asymmetry* **1999**, *10*, 671−674. (d) O'Brien, P. *Angew. Chem., Int. Ed.* **1999**, *38*, 326−329. (e) Bodkin, J. A.; McLeod, M. D. *J. Chem. Soc., Perkin Trans. 1* **2002**, 2733−2746.

10.1021/jo034178q CCC: $25.00
Published on Web 05/07/2003

SCHEME 1. Regioselectivity of Ring-Opening Reactions of Cyclic Sulfates and Epoxides

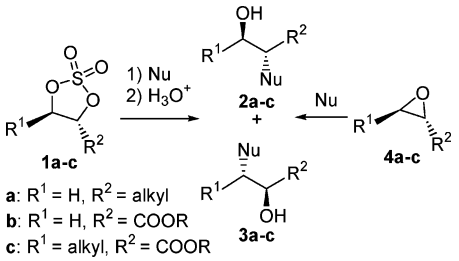

nant factor controlling the regioselectivity of the reaction (sulfate **1b** gives compound **2b**, Scheme 1).[9]

Moreover, a comparative study of regioselectivity in α,*β*-disubstituted cyclic sulfates and epoxides with various nucleophiles has shown that, when the ring-opening reaction is controlled by the electronic distribution of the substrates, the nucleophilic attack at the C_α position is again almost exclusive in the cyclic sulfates (sulfate **1c** gives compound **2c**, Scheme 1). On the other hand, with α,*β*-epoxyesters the attack occurs at either the C_α or C_β position depending on the reaction conditions used (epoxide **4c** gives compounds **2c** or **3c**, Scheme 1).[9b,c,10]

In contrast with these cases, little is known about the regioselectivity and stereoselectivity of *gem*-disubstituted α,*β*-cyclic sulfates. To the best of our knowledge, only two cases of reactions involving cyclic sulfates in which the *gem*-disubstituted carbon center is activated for nucleophilic attack have been reported. Goodman and co-workers[11] synthesized α,*β*-dimethyl-α-amino acids using as key steps the asymmetric dihydroxylation reaction of benzyl tiglate, followed by cyclic sulfate formation and a further stereoselective and regioselective ring-opening reaction with the azide ion at the C_α position of the cyclic sulfate. Avenoza and co-workers[12] used a similar protocol to achieve an enantioselective synthesis of both (*R*)- and (*S*)-α-methylserines.

To understand the behavior of this kind of cyclic sulfate in the ring-opening reaction with the azide ion and to shed light on the reaction mechanism and synthetic implications involved, we performed both experimental and theoretical studies. The results of this investigation are presented in this paper.

Computational Details

All calculations were carried out by means of the B3LYP hybrid functional.[13] Full optimizations and transition structure searches, using the 6-31+G(d) basis set, were carried out with the Gaussian 98 package.[14] BSSE corrections have not been considered in this work.

Analytical frequencies were calculated at the B3LYP/6-31+G(d) level and the nature of the stationary points was determined in each case according to the appropriate number of negative eigenvalues for the Hessian matrix. Scaled frequencies were not considered since significant errors on the calculated thermodynamical properties are not found at this theoretical level.[15]

In all cases single-point energy calculations at the B3LYP/6-311++G(2d,p) level were carried out on the B3LYP/6-31+G(d) geometries. Furthermore, solvent effects were taken into account through single-point energy calculations with the Isodensity Polarized Surface Continuum Model (IPCM) method,[16] as implemented in Gaussian 98, at the B3LYP/6-31+G(d) level, using the dielectric permittivity of dimethylformamide (38.25), which was the solvent used in most experiments. The IPCM method only accounts for the electrostatic part of the solvation energy, and not for dispersion and cavitation terms. However, as we are concerned only with relative energies, it is foreseeable that the *differential* solvation energy between two transition structures will be dominated by the electrostatic term, given the differences in electric moments (dipole and higher multipoles). On the other hand, dispersion and cavitation solvation energies (which have furthermore opposed signs) will tend to cancel out in these conditions. This behavior has been previously observed, for instance, in the case of Diels−Alder reactions.[17] Some single-point energy calculations were also carried out at the PCM/B3LYP/6-31+G(d) level, using nitromethane as the solvent, because of its close dielectric permittivity to dimethylformamide (38.2), to test the possible influence of cavitation and dispersion terms of the solvation energy, showing that our hypothesis about the cancellation of these terms is correct. Similarly, some single-point energy calculations were also carried out at the IPCM/B3LYP/6-311++G(2d,p) level, showing that the possible influence of the basis set size on the solvation energies is almost nil, therefore we decided to use the computationally more economical IPCM/B3LYP/6-31+G(d) level.

Natural Bonding Orbital (NBO)[18] analyses were carried out with use of the NBO 3.1 program, as implemented in Gaussian 98.

Unless otherwise stated, only Gibbs free energies are used for the discussion on the relative stabilities of the transition structures considered. These energies were obtained by using the following correction formula:

$$\Delta\Delta G^{\ddagger} = \Delta\Delta E_{\text{basis}} + \Delta\Delta G_{298} + \Delta\Delta G_{\text{solv}} \qquad (1)$$

where $\Delta\Delta E_{\text{basis}}$ is the relative energy at the B3LYP/6-311++G-

(8) (a) Kim, B. M.; Sharpless, K. B. *Tetrahedron Lett.* **1989**, *30*, 655−658. (b) He, L.; Byun, H.-S.; Bittman, R. *J. Org. Chem.* **1998**, *63*, 5696−5699. (c) Parkes, K. E. B.; Bushnell, D. J.; Crackett, P. H.; Dunsdon, S. J.; Freeman, A. C.; Gunn, M. P.; Hopkins, R. A.; Lambert, R. W.; Martin, J. A.; Merrett, J. H.; Redshaw, S.; Spurden, W. C.; Thomas, G. J. *J. Org. Chem.* **1994**, *59*, 3656−3664. (d) Yokumatsu, T.; Suemune, K.; Shibuya, S. *Heterocycles* **1993**, *35*, 577−580. (e) Hoffmann, R. W.; Stiasny, H. C. *Tetrahedron Lett.* **1995**, *36*, 4595−4598. (f) Hoye, T. R.; Crawford, K. B. *J. Org. Chem.* **1994**, *59*, 520−522.

(9) (a) Otsubo, K.; Inanaga, J.; Yamaguchi, M. *Tetrahedron Lett.* **1987**, *28*, 4435−4436. (b) Saito, S.; Takahashi, N.; Ishikawa, T.; Moriwaka, T. *Tetrahedron Lett.* **1991**, *32*, 667−670. (c) Righi, G.; Rumboldt, G.; Bonini, C. *J. Org. Chem.* **1996**, *61*, 3557−3560.

(10) Xiong, C.; Wang, W.; Hruby, V. J. *J. Org. Chem.* **2002**, *67*, 3514−3517.

(11) Shao, H.; Rueter, J. K.; Goodman, M. *J. Org. Chem.* **1998**, *63*, 5240−5244.

(12) Avenoza, A.; Cativiela, C.; Corzana, F.; Peregrina, J. M.; Sucunza, D.; Zurbano, M. M. *Tetrahedron*: *Asymmetry* **2001**, *12*, 949−957.

(13) (a) Lee, C.; Yang, W.; Parr, R. *Phys. Rev. B* **1988**, *37*, 785−789. (b) Becke, A. D. *J. Chem. Phys.* **1993**, *98*, 5648−5652.

(14) Frisch, M. J.; Trucks, G. W.; Schlegel, H. B.; Scuseria, G. E.; Robb, M. A.; Cheeseman, J. R.; Zakrzewski, V. G.; Montgomery, J. A., Jr.; Stratmann, R. E.; Burant, J. C.; Dapprich, S.; Millan, J. M.; Daniels, A. D.; Kudin, K. N.; Strain, M. C.; Farkas, O.; Tomasi, J.; Barone, V.; Cossi, M.; Cammi, R.; Mennucci, B.; Pomelli, C.; Adamo, C.; Clifford, S.; Ochterski, J.; Petersson, G. A.; Ayala, P. Y.; Cui, Q.; Morokuma, K.; Malick, D. K.; Rabuck, A. D.; Raghavachari, K.; Foresman, J. B.; Cioslowski, J.; Ortiz, J. V.; Stefanov, B. B.; Liu, G.; Liashenko, A.; Piskorz, P.; Komaroni, I.; Gomperts, R.; Martin, R. L.; Fox, D. J.; Keith, T.; Al-Laham, M. A.; Peng, C. Y.; Nanayakkara, A.; González, C.; Challacombe, M.; Gill, P. M. W.; Johnson, B.; Chen, W.; Replogle, E. S.; Pople, J. A. *Gaussian98*, Revisions A.7 and A.11; Gaussian, Inc.: Pittsburgh, PA, 1998.

(15) Bauschlicher, C. W., Jr. *Chem. Phys. Lett.* **1995**, *246*, 40−44.

(16) Foresman, J. B.; Keith, T. A.; Wiberg, K. B.; Snoonian, J.; Frisch, M. J. *J. Phys. Chem.* **1996**, *100*, 16098−16104.

(17) Ruiz-López, M. F.; Assfeld, X.; García, J. I.; Mayoral, J. A.; Salvatella L. *J. Am. Chem. Soc.* **1993**, *115*, 8780−8787.

(18) (a) Foster, J. P.; Weinhold, F. *J. Am. Chem. Soc.* **1980**, *102*, 7211−7218. (b) Reed, A. E.; Curtiss, L. A.; Weinhold, F. *Chem. Rev.* **1988**, *88*, 899−926. (c) Reed, A. E.; Weinstock, R. B.; Weinhold, F. *J. Chem. Phys.* **1985**, *83*, 735−746.

TABLE 1. Relative Energies, Free Energies (in kcal mol^{-1}), and Entropies (in cal K^{-1} mol^{-1}) for the Transition Structures Described in This Work

TS	ΔE_0[a]	ΔS[a]	$\Delta\Delta G_{298}$[a]	$\Delta\Delta G_{solv}$[b]	$\Delta\Delta E_{basis}$[c]	$\Delta\Delta G^{\ddagger}$[d]
13a_sf	0.00	142.0	0.00	0.00	0.00	**0.00**
13a_sh	0.76	138.0	1.43	2.28	0.36	4.07
13a_af	3.76	139.4	0.82	3.23	3.74	7.79
13a_ah	2.98	138.5	1.25	0.30	2.83	4.38
13b_sf	0.00	127.8	0.00	0.00	0.00	1.64
13b_sh	0.83	127.7	0.18	−0.18	0.42	2.06
13b_af	3.06	121.8	1.18	1.51	2.92	7.25
13b_ah	2.23	128.3	−0.06	−3.48	1.90	**0.00**
13c_sf	0.00	134.6	0.00	0.00	0.00	**0.00**
13c_sh	2.88	133.6	0.46	1.10	2.64	4.20
13c_af	6.23	135.7	−0.44	−4.30	6.10	1.36
13c_ah	5.43	133.3	0.54	−4.70	5.39	1.23

[a] Calculated at the B3LYP/6-31+G(d) level. [b] Calculated at the IPCM/B3LYP/6-31+G(d) level. [c] Calculated at the B3LYP/6-311++G(2d,p)//B3LYP/6-31+G(d) level. [d] Calculated with eq 1 (see Computational Details).

(2d,p)//B3LYP/6-31+G(d) level, $\Delta\Delta G_{298}$ represents the thermal and entropic corrections at 298 K, calculated at the B3LYP/6-31+G(d) level, and $\Delta\Delta G_{solv}$ is the solvation correction (relative solvation free energies), calculated at the IPCM/B3LYP/6-31+G(d) level.

The relative energies and free energies of the structures considered in this work are shown in Table 1. Hard data on Cartesian coordinates, electronic energies, as well as entropies, enthalpies, Gibbs free energies, and lowest frequencies of the different conformations of all structures considered, are available as Supporting Information.

Results and Discussion

1. Experimental Studies. Three different reactions were investigated: the ring-opening of cyclic sulfates **8a**−**c** with sodium azide under various conditions, which generate mixtures of compounds **9a**−**c** and **10a**−**c**. Subsequent acid hydrolyses gave the corresponding azido alcohols **11a**−**c** and **12a**−**c**.

Synthesis of Cyclic Sulfates. Olefins **5a** and **5c** were obtained from commercially available 2-methyl-2-propenoic acid, which was transformed into the corresponding 2-methyl-2-propionyl chloride by the action of PCl_5. Further in situ addition of methoxymethylamine or dimethylamine gave olefins **5a** or **5c**, respectively, according to the protocol described in the literature.[19] Olefin **5a** was subjected to the AD reaction in the presence of AD-mix β, giving diol **6a** with excellent enantiomeric excess according to the results obtained by Sharpless et al.[20] The amide group of this diol was transformed into the corresponding methyl ester group to obtain diol **6b** in two steps (basic hydrolysis with LiOH and subsequent esterification with AcCl in refluxing MeOH), as described in the literature.[12] Diol **6c** was obtained from olefin **5c** by dihydroxylation with OsO_4 in the presence of *N*-methylmorpholine *N*-oxide (NMO) (Scheme 2).

Diols **6a**−**c** were then transformed into the corresponding α,β-cyclic sulfites **7a**−**c** with thionyl chloride and subsequent oxidation of these sulfites with RuO_4, generated in situ, gave sulfates **8a**−**c** in good yields (Scheme 2).

SCHEME 2. Synthesis of Cyclic Sulfates 8a−c[a]

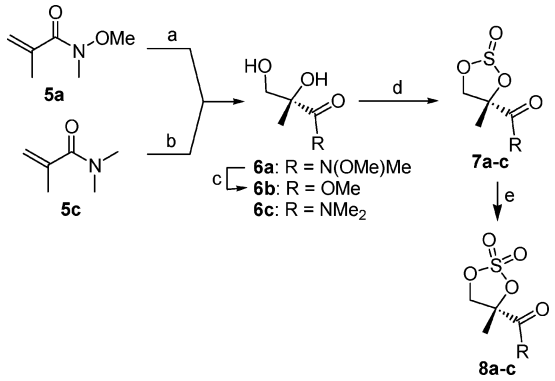

[a] Reagents and conditions: (a) AD-mix β, $MeSO_2NH_2$, ^{t}BuOH/H_2O (1:1), 0 °C, 12 h, 81%, ee 93%. (b) OsO_4, NMO, acetone/H_2O (4:1), rt, 24 h, 70%. (c) (i) LiOH·H_2O, H_2O/MeOH (1:3), rt, 2 h; (ii) AcCl, MeOH, reflux, 12 h, 85%. (d) $SOCl_2$, CCl_4, reflux, 4 h, 90% of **7a** from **6a**, 92% of **7b** from **6b**, 91% of **7c** from **6c**. (e) $NaIO_4$, $RuCl_3$, H_2O/MeCN/CCl_4 (3:2:2), 40 °C, 7 h, 92% of **8a** from **7a**, 86% of **8b** from **7b**, 77% of **8c** from **7c**.

SCHEME 3. Ring-Opening Reactions of Cyclic Sulfates 8a−c with the Azide Ion[a]

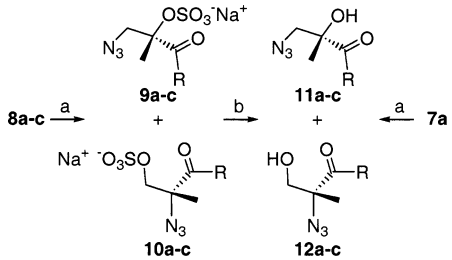

Sulfate	Method	R	9/10
8a	A	N(OMe)Me	3:1
8a	B	N(OMe)Me	4:1
8b	A	OMe	1:4.5
8c	A	NMe_2	6:1

[a] Reagents and conditions: (a) Method A: NaN_3, DMF, 50 °C, 48 h. Method B: NaN_3, acetone/H_2O (9:1), rt, 96 h. (b) 20% H_2SO_4, rt, 48 h.

Ring-Opening Reaction of Cyclic Sulfates. Sulfates **8a**−**c** were treated with sodium azide under various conditions to give mixtures of the acyclic sulfates **9a**−**c** and **10a**−**c**. These compounds could not be separated by column chromatography and were therefore immediately subjected to a further acid hydrolysis to give the corresponding azido alcohols **11a**−**c** and **12a**−**c** (Scheme 3).

When sulfate **8b** was treated with sodium azide in the presence of *N*,*N*-dimethylformamide (DMF) at 50 °C, a regioselectivity of 4.5:1 in favor of α-azido β-sulfate **10b** was obtained. This situation is in agreement with the results described previously.[12] Treatment of the reaction mixture (**9b** + **10b**) with 20% H_2SO_4 gave the corresponding mixture of azido alcohols (**11b** + **12b**), which could be separated by column chromatography (Scheme 3).

The regioselectivity of the reaction was measured from the crude reaction mixtures by integration of the ^{1}H NMR signals corresponding to the α-methyl group.

(19) Nahm, S.; Weinreb, S. M. *Tetrahedron Lett.* **1981**, *22*, 3815−3818.
(20) Bennani, Y. L.; Sharpless, K. B. *Tetrahedron Lett.* **1993**, *34*, 2079−2082.

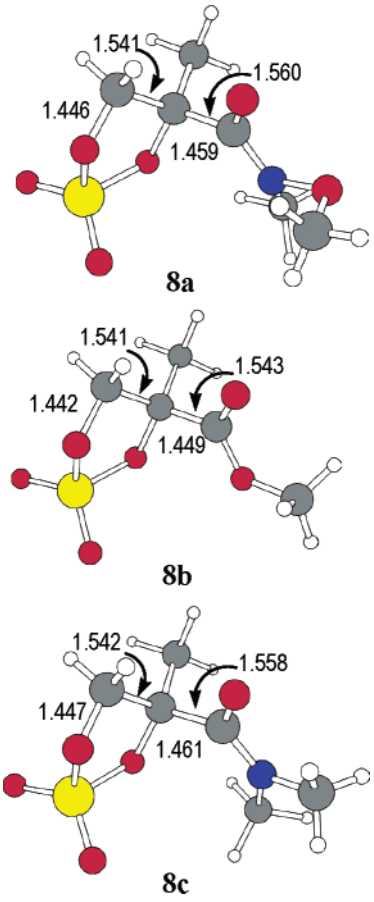

FIGURE 1. B3LYP/6-31+G(d) geometries of the minimum energy conformations of **8**a−**c**.

However, to our surprise, when sulfate **8a** was treated with sodium azide in the presence of *N*,*N*-dimethylformamide (DMF) at 50 °C, a regioselectivity of 3:1 in favor of *β*-azido α-sulfate **9a** was obtained. This regioselectivity was enhanced when the same reaction was carried out at room temperature in acetone/H_2O (9:1), although a time of 96 h was needed to complete the reaction. In this case the temperature could not be increased because at 50 °C we detected in the ^{1}H NMR spectrum a product arising from the nucleophilic attack of water. The regioselectivity of the opening reaction was determined in the final mixture of azido alcohols (**11a** + **12a**) prior to separation, using the same protocol as described above for the opening reaction of sulfate **8b** (Scheme 3). Alternatively, both azido alcohols were obtained by the ring-opening reaction of cyclic sulfite **7a**, under the same conditions (Method A), with the product mixture (**11a** + **12a**) obtained in 85% yield and with a regioselectivity of **11a**/**12a** = 5.5:1. These azido alcohols could be separated by column chromatography (Scheme 3).

In view of the results obtained on the regioselectivity of the ring-opening reaction of sulfate **8a**, it can be concluded that the reaction is not controlled by the electronic distribution of the substrate, a situation in stark contrast to the previously accepted position. To corroborate this feature, we carried out the ring-opening reaction of another cyclic sulfate, namely amide **8c**. In this case, nucleophilic attack of the azide ion on the sulfate **8c**, followed by hydrolysis, gave the mixture (**11c** + **12c**) in 91% yield and with a regioselectivity of **11c**/**12c** = 6:1, i.e. similar to that found for sulfate **8a** and opposite to that for sulfate **8b**. At first glance, the differences in electronic effects between the substituents in sulfates **8a**−**c** can hardly justify the almost complete reversal of regioselectivity observed. For this reason, we carried out a theoretical study of the reaction between sodium azide and these sulfates. Despite the importance of cyclic sulfates in organic synthesis there have not been any previous reports concerning computational studies on the ring-opening reaction with nucleophiles. Indeed, it is only recently that ab initio and DFT theoretical calculations regarding the solvent effects on the hydrolysis of simple model sulfates, including a cyclic structure, have been reported.[21] These reactions, however, follow a different mechanism since the nucleophilic attack takes place at the sulfur atom.

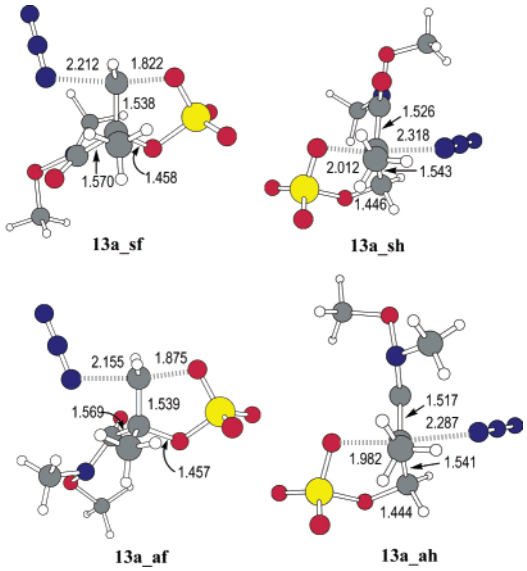

FIGURE 2. Some geometrical features of the TS **13a**, calculated at the B3LYP/6-31+G(d) level.

2. Theoretical Studies. Reactants. First, we calculated the structures of the reactants, the azide anion, and the three sulfates **8a**−**c**. Simplification of the structures of the sulfates was not considered to take into account all the steric interactions relevant in the transition structures. Some relevant features of the minimum energy conformations of **8a**−**c** are shown in Figure 1.

Transition Structures. For each sulfate **8a**−**c**, the corresponding transition structures (TS) resulting from nucleophilic attack of the azide anion on the C_α ("hindered") and C_β ("free") positions were located in the two possible carbonyl conformations, namely syn or anti with regard to the α-methyl group. This leads to four possible TS for each sulfate and these are denoted as **13a**−**c**_**sh**, **13a**−**c**_**ah**, **13a**−**c**_**sf**, and **13a**−**c**_**af**, respectively.

Several geometrical features of these TS are shown in Figures 2−4 and the energetic results are gathered in Table 1.

A number of geometrical features can be established for transition structures **13a** (Figure 2). On one hand,

(21) (a) Lopez, X.; Dejaegere, A.; Karplus, M. *J. Am. Chem. Soc.* **2001**, *123*, 11755−11763. (b) Lopez, X.; Dejaegere, A.; Karplus, M. *J. Am. Chem. Soc.* **1999**, *121*, 5548−5558.

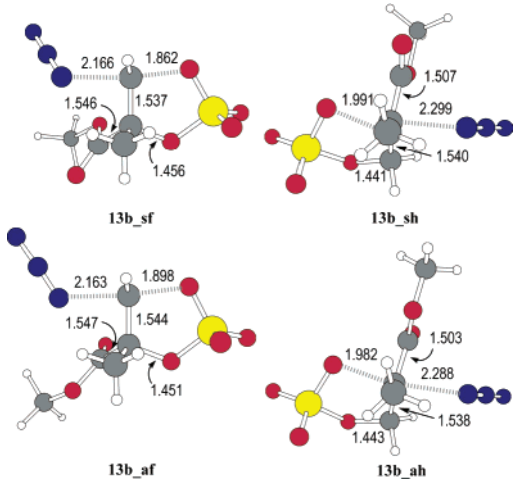

FIGURE 3. Some geometrical features of the TS **13b**, calculated at the B3LYP/6-31+G(d) level.

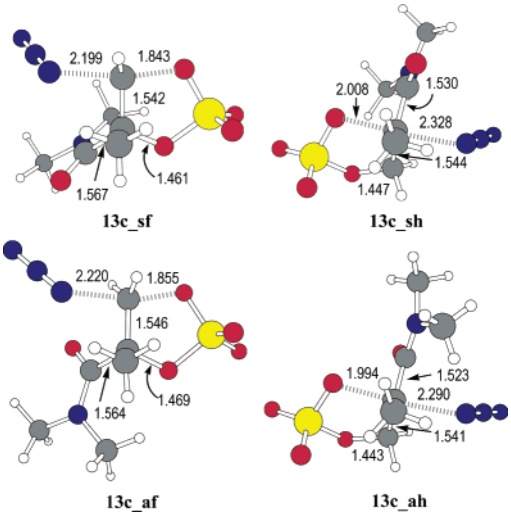

FIGURE 4. Some geometrical features of the TS **13c**, calculated at the B3LYP/6-31+G(d) level.

the N−C distances of the forming bonds are shorter in the case of nucleophilic attack at the less-hindered C_β position (**13a_sf** and **13a_af**). This could be interpreted in terms of these TS being later in the reaction coordinate, although the distances of the C−O breaking bond are also shorter for **13a_sf** and **13a_af**, which would indicate an earlier position in the reaction coordinate. In fact, it can be concluded that both **13a_sf** and **13a_af** TS are more compressed than **13a_sh** and **13a_ah**. This situation can be explained by steric effects, which must be more important in the case of nucleophilic attack at the most hindered position (**13a_sh** and **13a_ah**), resulting in a longer N−C distance in the TS. Natural population analyses of the TS allow further clarification of this point. Thus, the charge transfer from the azide anion to the sulfate in the TS is 0.312 and 0.349 electrons respectively for **13a_sf** and **13a_af**, whereas it is 0.382 and 0.393 for **13a_sh** and **13a_ah**, respectively. This is consistent with a later TS for nucleophilic attack at the most hindered C_α position. Therefore, if a single geometrical feature is to be chosen as a rapid indication of the earliness of the TS, the C−O breaking bond distance seems to be more reliable.

As far as the relative energies of the four TS are concerned (Table 1), it can be seen that **13a_sf** is the lowest energy TS both in the gas phase and in solution. The basis set effect seems to be less important in describing the relative energy of the TS, since the values calculated at the B3LYP/6-31+G(d) level and those calculated at the B3LYP/6-311++G(2d,p)//B3LYP/6-31+G(d) level are very similar. Both the thermal and solvation corrections follow the same trend in favoring **13a_sf** over the rest of the TS. Thus, the energy difference between nucleophilic attack at the less and the more hindered positions is calculated to be greater than 4 kcal mol^{-1}, which is in qualitative agreement with the high regioselectivity observed in the reactions of **8a**.

In transition structures **13b** (Figure 3) the same features as described for TS **13a** are reproduced. Thus, the C−O breaking bond distance is shorter for **13b_sf** and **13b_af**, indicating an earlier TS for the nucleophilic attack at the less-hindered position. The natural population analysis also agrees with this conclusion, since the charge transfer is lower for these TS when compared with **13b_sh** and **13b_ah** (0.345 and 0.342 for **13b_sf** and **13b_af**, and 0.386 and 0.400 for **13b_sh** and **13b_ah**, respectively). On the other hand, and in a similar way to that found for TS **13a**, the N−C bond-forming distance is longer in the case of **13b_sh** and **13b_ah**, which can be attributed to greater steric interactions in these TS.

From the energy viewpoint, the gas-phase calculations lead to conclusions similar to those found for TS **13a**, i.e., **13b_sf** is the lowest energy TS, showing that the intrinsic stereoelectronic effects are in the same sense for both kinds of structures. However, the situation dramatically changes when solvent effects are taken into account. The TS **13b_ah** is preferentially solvated in comparison to **13b_sf** by ca. 3.5 kcal mol^{-1}. This preferential solvation leads to a reverse regioselectivity for this reaction, with nucleophilic attack at the most hindered C_α position now being favored by ca. 1.6 kcal mol^{-1}, which is again in qualitative agreement with the experimental results.

As a referee noted, solvation effects may be sensitive to the basis set size. Given that solvation is so critical in determining the relative stability of these TS, we carried out single-point energy calculations at the IPCM/B3LYP/6-311++G(2d,p) level for **13b_ah** and **13b_sf**. The qualitative conclusions reached with the 6-31+G(d) basis set do not change, and thus, the preferential solvation of **13b_ah** is ca. 2.6 kcal mol^{-1}, whereas this TS is lower in energy than **13b_sf** by ca. 0.8 kcal mol^{-1}, when all the energy corrections are taken into account.

Another possible source of error in correctly assigning the role of the solvent in the regioselectivity is the neglect of cavitation and dispersion terms of the solvation energy by the IPCM method. To test this point, single-point energy calculations were carried out at the PCM/B3LYP/6-31+G(d) level for **13b_ah** and **13b_sf**. Unfortunately, dimethylformamide is not parametrized in Gaussian 98, so that these solvation terms cannot be calculated for this solvent. We then considered nitromethane as a reasonable substitute, because it is parametrized, and has the same dielectric permittivity (38.2) as dimethylformamide, so that the electrostatic component of the solvation energy will be essentially the same. The results obtained are shown in Table 2.

TABLE 2. PCM/B3LYP/6-31+G(d) Calculated Solvation Energy Terms (in kcal mol^{-1}) for Two Selected TS

TS	E_{Elec}	ΔE_{Elec}	E_{Cav}	ΔE_{Cav}	E_{Disp}	ΔE_{Disp}
13b_sf	−42.21	0.00	23.89	0.00	−22.74	0.00
13b_ah	−43.73	−1.52	23.96	0.07	−22.74	0.00

TABLE 3. Charge Transfer from the Azide Anion to the Sulfate Reactant in the TS, Calculated from Natural Population Analyses, at the B3LYP/6-31+G(d) (gas phase) and IPCM/B3LYP/6-31+G(d) (solution) Levels

TS	gas phase	solution
13a_sf	0.312	0.279
13a_ah	0.393	0.390
13b_sf	0.345	0.341
13b_ah	0.400	0.345
13c_sf	0.321	0.312
13c_ah	0.376	0.353

As can be seen, in agreement with our former hypothesis, the cavitation and dispersion terms cancel out almost perfectly, so that the differential solvation energy between both TS is practically the same as the differential electrostatic solvation energy, which is, in turn, very similar to the value calculated at the IPCM/B3LYP/6-31+G(d) level.

In transition structures **13c** (Figure 4) the same geometrical features as described for TS **13a** and **13b** are reproduced. Therefore, in principle, it can be concluded that the three sulfates have the same intrinsic behavior from a mechanistic point of view.

In terms of energy, TS **13c** shares some features of both **13a** and **13b**. Thus, the results of gas-phase calculations show that **13c_sf** is the lowest energy TS, which is analogous to the situation found for TS **13a** and **13b**. Furthermore, the differential solvation favors TS **13c_ah** over **13c_sf**, again in an analogous way to **13b**. However, contrary to the latter TS, this differential solvation is not sufficiently high to reverse the relative stability of the two TS, and therefore **13c_sf** continues to be the lowest energy TS even when solvation effects are taken into account.

It can be concluded that the intrinsic features of the TS for the three sulfates are very similar, which indicates similar stereoelectronic effects acting in all cases. However, there are important subtle changes due to the different electronic effects of the sulfate substituents, and these result in differential stabilization of one or another TS because of solvent effects. The natural population analysis of the TS, both in the gas phase and in solution, sheds some light on this point. The most relevant results are shown in Table 3.

As can be seen, the behavior of the charge transfer follows the observed solvation pattern. Thus, in the case of **13a_ah**, the charge transfer is almost the same in both the gas phase and solution, whereas it is smaller for **13a_sf** in solution than in the gas phase. This results in a preferential solvation of the latter due to a greater charge localization. The situation is reversed for TS **13b** and **13c**. Here, TS **13b_ah** and **13c_ah** show smaller charge-transfer values in solution than in the gas phase, as compared with **13b_sf** and **13c_sf**, thus resulting in preferential solvation of the former.

It can be argued that, under these conditions, solvent effects must also be relevant for the position of the TS in the reaction coordinate. Although we believe that this is the case, we think that the reoptimization of the TS in the presence of the reaction field will result in an enhancement of solvent effects, as already demonstrated in other cases,[17,22] but will not cause changes in the relative stability of the TS with regard to that observed in the single-point energy calculations.

Experimental support would also help to clarify the role of solvent effects on the regioselectivity of these reactions. On one hand, the reaction of **8b** in solvents that are less polar than DMF should lead to lower or even reverse regioselectivity as a result of a lower differential solvation of **13b_ah**. Several experiments were carried out with acetone ($\epsilon = 20.70$), but the solubility of the sodium azide was too low in this solvent and the reaction does not proceed at an appreciable rate. On the other hand, reaction of **8c** in solvents that are more polar than DMF should also lead to lower regioselectivity, this time due to a greater differential solvation of **13c_ah**. A reaction carried out in dimethyl sulfoxide (DMSO, $\epsilon = 46.68$) led to a regioselectivity of 5:1, somewhat lower than the 6:1 observed in DMF. When the dielectric permittivity of the solvent was further increased by using *N*-methyl formamide ($\epsilon = 182.4$), the regioselectivity dropped to 3.6:1. The linear correlation between the Kirkwood function[23] $(\epsilon - 1)/(2\epsilon + 1)$ and the $\Delta\Delta G$ calculated at 298 K from the experimental regioselectivity values is excellent ($r = 0.990$). These results do support the conclusions reached from the theoretical study. Unfortunately, solubility of the reagents and low nucleophilicity of the solvent are two prerequisite conditions and these limit the choice of solvents for an experimental investigation into the key role of solvent effects on the regioselectivity of these reactions.

Conclusions

The regioselectivity of the nucleophilic ring-opening reactions of three *gem*-disubstituted cyclic sulfates with sodium azide depends on the substituent present in the cyclic sulfate. Amide substituents lead preferentially to products arising from nucleophilic attack at the least-substituted C_β position, whereas reverse regioselectivity is obtained with ester substituents. This is advantageous from a synthetic point of view, since it allows one or another regioisomer to be obtained preferentially with selectivities greater than 4:1.

Theoretical calculations show that, contrary to the previously accepted situation, the intrinsic preference in all cases is for azide attack at the least-substituted C_β position on the basis of similar stereoelectronic effects acting on the TS of the three sulfates considered. The observed preference for C_α attack in the case of the ester sulfate is explained in terms of differential solvent effects, which are in turn due to subtle differences in the charge transfer of the different transition structures.

Experimental Section

General Procedures. Unless otherwise stated, all starting materials were obtained from commercial suppliers and used without further purification. Melting points are uncorrected.

(22) Assfeld, X.; Ruiz-López, M. F.; García, J. I.; Mayoral, J. A.; Salvatella, L. *J. Chem. Soc., Chem. Commun.* **1995**, 1371−1372.
(23) Kirkwood, J. G. *J. Chem. Phys.* **1934**, *2*, 351−361.

All manipulations involving air-sensitive reagents were carried out under a dry argon atmosphere with standard Schlenk techniques. Solvents were purified according to standard procedures. Analytical TLC was performed with use of precoated plastic sheets of 40 × 80 mm^2. Column chromatography was performed with silica gel 60 (230−400 mesh). Organic solutions were dried over anhydrous Na_2SO_4 and, when necessary, concentrated under reduced pressure by using a rotary evaporator. NMR spectra were recorded at 300 MHz (^{1}H) and at 75 MHz (^{13}C) and are reported in ppm downfield from TMS. Microanalyses were in good agreement with the calculated values. Mass spectra were obtained by electrospray ionization (ESI).

General Procedure for the Generation of Cyclic Sulfites. The corresponding diol **6** (32.8 mmol) was dissolved in CCl_4 (60 mL) and $SOCl_2$ (7.74 g, 42.6 mmol) was then added. The resulting solution was heated under reflux for 4 h. The solvent and excess $SOCl_2$ were evaporated and the crude product was purified by column chromatography to give the corresponding sulfite **7** as a colorless liquid.

General Procedure for the Generation of Cyclic Sulfates. Compound **7** (2.78 mmol) was dissolved in a mixture of water (15 mL), MeCN (10 mL), and CCl_4 (10 mL). $NaIO_4$ (1.16 g, 5.42 mmol) and $RuCl_3$ hydrate (10 mg, 0.05 mmol) were added and the solution was vigorously stirred for 7 h at 40 °C. Ethyl ether (75 mL) was added to the cooled mixture. The organic layer was removed, dried (Na_2SO_4), and concentrated. The crude product was chromatographed to give the corresponding compound **8** as a colorless liquid.

General Procedure for Ring-Opening Reactions of Sulfites. To a solution of cyclic sulfite **7** (31.6 mmol) in DMF (30 mL) was added NaN_3 (2.72 g, 41.8 mmol). The mixture was stirred at 50 °C for 48 h to give a mixture of azido alcohols **11** and **12**. The solvent was removed and the residue partitioned between H_2O (30 mL) and ethyl acetate (70 mL). The aqueous layer was successively washed with ethyl acetate (4 × 40 mL), the combined organic layers were dried (Na_2SO_4) and concentrated, and the crude product was chromatographed to give *β*-azido α-alcohol **11** and α-azido *β*-alcohol **12** as colorless liquids.

General Procedure for Ring-Opening Reactions of Sulfates. Method A: To a stirred solution of cyclic sulfate **8** (31.6 mmol) in DMF (30 mL) was added NaN_3 (2.72 g, 41.8 mmol). The mixture was stirred at 50 °C for 2 d to give a mixture of acyclic azido sulfates **9** and **10**. The reaction was concentrated under reduced pressure, ethyl ether (30 mL) and water (1 mL) were added, and the solution was chilled to 0 °C. Aqueous H_2SO_4 (20%; 3 mL) was added and the solution was vigorously stirred at room temperature for 2 d. The organic layer was collected and concentrated, and the crude product was chromatographed to give *β*-azido α-alcohol **11** and α-azido *β*-alcohol **12** as colorless liquids. **Method B:** To a solution of cyclic sulfate **8** (2.14 mmol) in acetone (20 mL) and water (2 mL) was added NaN_3 (0.35 g, 5.38 mmol). The mixture was stirred at room temperature for 96 h to give a mixture of acyclic azido sulfates **9** and **10**. Compounds **11** and **12** were obtained following the same protocol as described above for Method A.

2,3-Dihydroxy-2,*N*,*N*-trimethylpropionamide (6c). To a solution of **5c** (0.95 g, 8.41 mmol) in acetone/H_2O (4:1) (68 mL) at 0 °C were added NMO (4.90 g, 42.05 mmol) and OsO_4 (9 mL, 0.84 mmol, 2.5% w). The mixture was stirred at room temperature for 24 h. The acetone was evaporated and the residue partitioned between H_2O (30 mL) and ethyl acetate (70 mL). The aqueous layer was washed with ethyl acetate (4 × 40 mL), the combined organic extracts were dried (Na_2SO_4) and concentrated, and the crude product was chromatographed with methanol/ethyl acetate (5:95) to give diol **6c** as an oil (70%). ^{1}H NMR ($CDCl_3$) *δ* 1.33 (s, 3H), 2.93 (br s, 3H), 3.20 (br s, 3H), 3.39 (d, 1H, *J* = 12.0 Hz), 3.94 (d, 1H, *J* = 12.0 Hz), 4.36 (br s, 2H). ^{13}C NMR ($CDCl_3$) *δ* 14.0, 21.4, 60.3, 69.2, 174.0. Anal. Calcd for $C_6H_{13}NO_3$: C, 48.97; H, 8.90; N, 9.52. Found: C, 48.79; H, 8.98; N, 9.60.

(*S*)-4-Methyl-2-oxo-2*λ*^{4}-[1,3,2]dioxathiolane-4-carboxylic Acid *N*-Methoxy-*N*-methylamide (7a). Column chromatography on silica gel, eluting with hexane/ethyl acetate (6:4), gave 6.19 g of sulfite **7a** of *S*-configuration (90%). $[\alpha]^{25}_D$ +36.6 (*c* 1.04, MeOH). ^{1}H NMR ($CDCl_3$) *δ* 1.52 (s, 3H), 1.77 (s, 3H), 3.06−3.16 (m, 6H), 3.66 (s, 6H), 4.20 (d, 1H, *J* = 9.0 Hz), 4.35 (d, 1H, *J* = 9.0 Hz), 5.10 (d, 1H, *J* = 3.6 Hz), 5.13 (d, 1H, *J* = 3.6 Hz). ^{13}C NMR ($CDCl_3$) *δ* 21.8, 22.3, 33.0, 61.1, 73.3, 73.9, 87.8, 89.1, 168.0. ESI$^+$ (*m*/*z*) 210. Anal. Calcd for $C_6H_{11}NO_5S$: C, 34.44; H, 5.30; N, 6.69. Found: C, 34.37; H, 5.33; N, 6.65. Duplication of some signals was observed in the ^{1}H and ^{13}C NMR spectra, indicating the existence of two conformers in solution.

4-Methyl-2-oxo-2*λ*^{4}-[1,3,2]dioxathiolane-4-carboxylic Acid *N*,*N*-Dimethylamide (7c). Column chromatography on silica gel, eluting with hexane/ethyl acetate (1:1), gave 5.72 g of sulfite **7c** (91%). ^{1}H NMR ($CDCl_3$) *δ* 1.58 (s, 3H), 1.78 (s, 3H), 2.85−2.93 (m, 6H), 3.10−3.20 (m, 6H), 4.25 (d, 1H, *J* = 9.0 Hz), 4.37 (d, 1H, *J* = 9.0 Hz), 5.20 (d, 1H, *J* = 3.6 Hz), 5.34 (d, 1H, *J* = 3.6 Hz). ^{13}C NMR ($CDCl_3$) *δ* 22.9, 23.3, 36.8, 37.2, 37.8, 37.9, 75.1, 75.2, 88.5, 89.4, 168.1, 168.6. Anal. Calcd for $C_6H_{11}NO_4S$: C, 37.30; H, 5.74; N, 7.25. Found: C, 37.47; H, 5.73; N, 7.28. Duplication of some signals was observed in the ^{1}H and ^{13}C NMR spectra, indicating the existence of two conformers in solution.

(*S*)-4-Methyl-2,2-dioxo-2*λ*^{6}-[1,3,2]dioxathiolane-4-carboxylic Acid *N*-Methoxy-*N*-methylamide (8a). Column chromatography on silica gel, eluting with hexane/ethyl acetate (6:4), gave 576 mg of sulfate **8a** of *S*-configuration (92%). $[\alpha]^{22}_D$ +8.1 (*c* 0.65, MeOH). ^{1}H NMR ($CDCl_3$) *δ* 1.83 (s, 3H), 3.25 (s, 3H), 3.78 (s, 3H), 4.41 (d, 1H, *J* = 9.0 Hz), 5.31 (d, 1H, *J* = 9.0 Hz). ^{13}C NMR ($CDCl_3$) *δ* 21.4, 32.9, 61.5, 75.3, 88.0, 166.6. ESI$^+$ (*m*/*z*) 226. Anal. Calcd for $C_6H_{11}NO_6S$: C, 32.00; H, 4.92; N, 6.22. Found: C, 31.87; H, 4.91; N, 6.19.

4-Methyl-2,2-dioxo-2*λ*^{6}-[1,3,2]dioxathiolane-4-carboxylic Acid *N*,*N*-Dimethylamide (8c). Column chromatography on silica gel, eluting with hexane/ethyl acetate (1:1), gave 448 mg of sulfate **8c** (77%). ^{1}H NMR ($CDCl_3$) *δ* 1.80 (s, 3H), 2.98 (s, 3H), 3.16 (s, 3H), 4.45 (d, 1H, *J* = 9.3 Hz), 5.24 (d, 1H, *J* = 9.3 Hz). ^{13}C NMR ($CDCl_3$) *δ* 22.4, 37.1, 37.6, 76.7, 88.3, 166.5. Anal. Calcd for $C_6H_{11}NO_5S$: C, 34.44; H, 5.30; N, 6.69. Found: C, 34.41; H, 5.38; N, 6.63.

(*S*)-3-Azido-2-hydroxy-*N*-methoxy-2,*N*-dimethylpropionamide (11a). Starting from sulfite **7a** and after column chromatography on silica gel, eluting with hexane/ethyl acetate (3:7), 4.55 g of *β*-azido α-alcohol (*S*)-**11a** (76%) was obtained. Compound (*S*)-**11a**: $[\alpha]^{24}_D$ −68.9 (*c* 1.97, MeOH). ^{1}H NMR ($CDCl_3$) *δ* 1.41 (s, 3H), 3.28 (s, 3H), 3.45−3.50 (m, 2H), 3.70 (s, 3H). ^{13}C NMR ($CDCl_3$) *δ* 22.8, 33.5, 57.4, 60.9, 75.8, 173.6. ESI$^+$ (*m*/*z*) 188 + Na. Anal. Calcd for $C_6H_{12}N_4O_3$: C, 38.29; H, 6.43; N, 29.77. Found: C, 38.21; H, 6.41; N, 29.71.

(*R*)-2-Azido-3-hydroxy-*N*-methoxy-2,*N*-dimethylpropionamide (12a). Starting from sulfite **7a** and after column chromatography on silica gel, eluting with hexane/ethyl acetate (3:7), 803 mg of α-azido *β*-alcohol (*R*)-**12a** (13%) was obtained. $[\alpha]^{22}_D$ +61.6 (*c* 0.96, MeOH). ^{1}H NMR ($CDCl_3$) *δ* 1.50 (s, 3H), 3.22 (s, 3H), 3.55−3.85 (m, 5H). ^{13}C NMR ($CDCl_3$) *δ* 17.6, 33.2, 60.9, 66.6, 68.6, 171.6. ESI$^+$ (*m*/*z*) 188 + Na. Anal. Calcd for $C_6H_{12}N_4O_3$: C, 38.29; H, 6.43; N, 29.77. Found: C, 38.20; H, 6.42; N, 29.74.

3-Azido-2-hydroxy-2,*N*,*N*-trimethylpropionamide (11c). Starting from sulfate **8c** and after column chromatography on silica gel, eluting with hexane/ethyl acetate (1:1), 291 mg of *β*-azido α-alcohol **11c** (79%) was obtained. Compound **11c**: ^{1}H NMR ($CDCl_3$) *δ* 1.44 (s, 3H), 2.90−3.19 (m, 6H), 3.40 (d, 1H, *J* = 12.6 Hz), 3.64 (d, 1H, *J* = 12.6 Hz). ^{13}C NMR ($CDCl_3$) *δ* 23.2, 38.0, 58.8, 75.4, 172.9. Anal. Calcd for $C_6H_{12}N_4O_2$: C, 41.85; H, 7.02; N, 32.54. Found: C, 41.79; H, 7.04; N, 32.59.

2-Azido-3-hydroxy-2,*N*,*N*-trimethylpropionamide (12c). Starting from sulfate **8c** and after column chromatography on

silica gel, eluting with hexane/ethyl acetate (1:1), α-azido *β*-alcohol **12c** was obtained as a mixture with **11c**. Compound **12c**: ^{1}H NMR ($CDCl_3$) δ 1.35 (s, 3H), 2.95−3.26 (m, 6H), 3.77 (d, 1H, J = 12.3 Hz), 3.98 (d, 1H, J = 12.3 Hz).

Acknowledgment. We thank the Ministerio de Ciencia y Tecnología (projects PPQ2001-1305 and PPQ2002-04012), Gobierno de La Rioja (project ANGI-2001/30), and Universidad de La Rioja (project API-01/B02) for financial support.

Supporting Information Available: Tables of electronic energies, as well as entropies, Gibbs free energies (the last three data series at 25 °C), lowest frequencies, and Cartesian coordinates for the different conformations of the structures considered in this work. This material is available free of charge via the Internet at http://pubs.acs.org.

JO034178Q